ChemComm

COMMUNICATION

High capacity Na-storage and superior cyclability of nanocomposite Sb/C anode for Na-ion batteries†

Jiangfeng Qian, Yao Chen, Lin Wu, Yuliang Cao, Xinping Ai and Hanxi Yang*

A Sb/C nanocomposite was synthesized and found to deliver a reversible 3 Na storage capacity of 610 mA h g^{-1}, a strong rate capability at a very high current of 2000 mA g^{-1} and a long-term cycling stability with 94% capacity retention over 100 cycles, offering practical feasibility as a high capacity and cycling-stable anode for room temperature Na-ion batteries.

Rechargeable Na-based batteries have long been pursued as the most attractive alternative to Li-ion batteries for electric vehicle propulsion and renewable electric power storage because of their potential advantages of low cost and the widespread availability of sodium resources.[1–3] Also, from the electrochemical point of view, sodium has a very negative redox potential (−2.71 V, *vs.* SHE) and a small electrochemical equivalent (0.86 g A h^{-1}), which make it the most advantageous element for battery applications after lithium. Despite many encouraging works that have been done on Na-based battery chemistry in past decades, only high-temperature Na/S and Na/NiCl$_2$ (ZEBRA battery) systems have been commercially developed for electric vehicles and MWh scale electric storage. A major obstacle hindering the broad market penetration of these Na batteries is the long term stability and endurance of the battery components at the high temperatures of $\geq 300\,^{\circ}$C.[4] If a room temperature Na$^+$ ion rocking chair battery (Na-ion battery) can be achieved, it would bring about a great improvement in the safety and operational simplicity with respect to conventional high temperature Na batteries and also a remarkable decrease in cost with regard to Li-ion batteries, thus ensuring sustainable applications for large scale electric energy storage.

To realize Na-ion technology, a variety of sodium host cathodes (positive electrode) have been reported to have certain Na-storage capacity and cycleability.[5–9] In contrast, the anodic (negative) host materials have been less successfully developed with the majority of works devoted to carbonaceous materials,[10–12] due to a frustrated insertion of larger Na$^+$ ions in graphitic layers.

A well-accepted strategy in the recent development of safer and high capacity Li-storage anodes is to use metallic and intermetallic

anodic host materials as substitutes for the graphite anode. This strategy could also be applied to develop Na-storage anode materials. In fact, Na can also alloy with some Group IVA and VA elements, such as Sn, Pb, Sb and P, to form intermetallic compounds[13] with very high Na-storage capacities, such as Na$_{15}$Sn$_4$ (847 mA h g^{-1}), Na$_{15}$Pb$_4$ (485 mA h g^{-1}), Na$_3$Sb (660 mA h g^{-1}) and Na$_3$P (2560 mA h g^{-1}). However, there have been only a few research studies on these alloy compounds for reversible Na-storage anodes up to date. Very recently, Xiao *et al.*[14] reported a SnSb/C alloy anode for Na-ion batteries, which gave an initial capacity of over 500 mA h g^{-1}, but cycled with a gradual decrease in the reversible capacity during 50 cycles.

Herein, we demonstrate a highly reversible Na alloying reaction on a Sb/C nanocomposite with a nearly three Na insertion capacity of 610 mA h g^{-1} and a $>$90% capacity retention over 100 cycles, which offers a new alternative to carbonaceous Na hosts as a high capacity and safer anodic material for Na-ion batteries.

The Sb/C nanocomposites were simply prepared by mechanical milling of commercial Sb powder with super P carbon (for experimental details, see ESI†). The XRD pattern of the as prepared Sb/C composite is shown in Fig. 1a. Although they are weak and broad, all of the XRD signals of the Sb/C composite can be traced to a rhombohedral phase of Sb ($R\bar{3}m$ 166). Using Scherer's formula, the mean crystallite size of the Sb particles in the composite was calculated to be about 10 nm. An SEM image (Fig. 1b) shows a morphological feature of the Sb/C composite appearing as irregular aggregates several hundreds of nanometers in size. The high resolution TEM image in Fig. 1c clearly shows the lattice fringes of 0.344 nm in dispersed dots of $\phi \approx 10$ nm, corresponding to the *d* spacing value of the (012) plane of hexagonal Sb, revealing that the Sb/C particles are composed of $\sim$10 nm nanocrystallite Sb embedded in the carbon matrix. Such a composite structure is favorable to tolerate the massive volume changes of the Sb phase during Na alloying/dealloying reaction ($\sim$390% volume expansion from Sb to Na$_3$Sb lattice), due to the downsizing of Sb particles and buffering effect of the carbon matrix.

The electrochemical properties of reversible Na alloying reaction on the Sb/C composite in 1.0 mol L^{-1} NaPF$_6$ EC-DEC solution are demonstrated in Fig. 2. The cyclic voltammograms (CV, Fig. 2a) of the Sb/C electrode display two pairs of well-defined symmetric redox bands at 0.65/0.93 V

College of Chemistry and Molecular Science, Wuhan University, Wuhan 430072, China. E-mail: hxyang@whu.edu.cn; Fax: +86-27-87884476; Tel: +86-27-87884476
† Electronic supplementary information (ESI) available: Experimental details, electrochemical characterization, *ex situ* XRD patterns and EIS spectra of the Sb/C anodes. See DOI: 10.1039/c2cc32730a

Fig. 1 (a) X-ray diffraction patterns of the Sb/C nanocomposite and metallic Sb. (b and c) SEM and HRTEM images of the Sb/C nanocomposite.

and 0.40/0.78 V, respectively, suggesting two steps of Na alloying/dealloying reactions occurring on the Sb/C electrode. Considering that binary Na–Sb alloys exist preferably in two stable NaSb and Na_3Sb phases and that the area ratio of the two pairs of CV bands is close to 3:1, the two pairs of redox bands can be attributed to the formation of NaSb and Na_3Sb as follows:

$$Sb \ (rhom) + Na^+ + e^- \leftrightarrow NaSb \ (mono) \qquad (1)$$

$$NaSb \ (mono) + 2 \ Na^+ + 2e^- \leftrightarrow Na_3Sb \ (hex) \qquad (2)$$

Fig. 2b shows the charge/discharge performance of the Sb/C composite. All of the capacities of the Sb/C composite in this paper were calculated on the basis of the mass of Sb and the capacity contribution from the carbon is excluded (see ESI, Fig. S1†). As shown in Fig. 2b, the potential profiles show two distinguishable plateaus at $+0.56$ V$/+0.37$ V at charge (Na alloying) and $+0.74$ V$/0.92$ V at discharge (Na dealloying), which agree very well with the potential positions of the CV bands in Fig. 2a. The initial discharge capacity of the Sb/C anode reaches 610 mA h g^{-1}, considerably exceeding a 2 Na storage and approaching a 3 Na storage capacity (Na_3Sb: 660 mA h g^{-1}). Though the CV and charge–discharge evidences point out a two-step Na alloying reaction on the Sb/C anode, unfortunately, we failed to detect the phase change of the Na_xSb (x = 1–3) at different depths of charge and discharge (see ESI, Fig. S2†) due to the loss of the crystallinity of the Sb/C nanocomposite at the small nanoscale. This could be attributed to a rapid amorphization and the subsequent apparent solid solution behavior of the electrode material.

In contrast to metallic Sb powders, the Sb/C nanocomposite shows greatly enhanced cycling stability (see ESI, Fig. S3†). Though the pure Sb powders can deliver a high initial capacity of 624 mA h g^{-1}, its capacities decreased very rapidly down

Fig. 2 Electrochemical properties of the Sb/C nanocomposite: (a) The CV curve at a scan rate of 0.1 mV s^{-1} (vs. Na$^+$/Na); (b) charge–discharge curves of the Sb/C composite at a constant current of 100 mA g^{-1}, the inset is differential capacity versus cell potential curve; (c) charge–discharge profiles at various current densities from 150 mA g^{-1} to 2000 mA g^{-1}.

to <100 mA h g^{-1} only after 25 cycles. Nevertheless, the Sb/C nanocomposite shows an initial charge/discharge capacities of 717/610 mA h g^{-1}, giving a high initial coulombic efficiency of 85%. Since the 2nd cycle, the reversible capacity kept stable at $\sim$580 mA h g^{-1} and the coulombic efficiency increased to 99% at subsequent cycles. This reversible capacity corresponds to a 90% utilization of its theoretical 3 Na storage capacity of the active Sb phase during prolonged cycling.

In addition to the high capacity and cyclability, the Sb/C electrode also exhibits remarkable high-rate capability. Fig. 2d shows the rate performance of the Sb/C nanocomposite. The electrode delivers a discharge capacity of 546 mA h g^{-1}, 489 mA h g^{-1} and 382 mA h g^{-1} at high rates of 500, 1000 and 1500 mA g^{-1}, respectively. Even at a very high rate of 2000 mA g^{-1}, the reversible capacity can still reach 309 mA h g^{-1}, 50% of its realizable capacity, demonstrating the facile kinetics of the Na alloying/dealloying reactions.
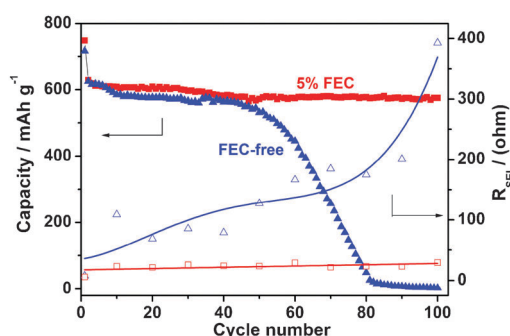
Fig. 3 Changes of the cycling capacities and SEI film resistances of the Sb/C anodes in the 1.0 mol L^{-1} NaPF$_6$ + EC-DEC electrolyte with (red ■ □) and without (blue ▲ △) the addition of 5% FEC additive.

To evaluate the long-term cycling stability of the Sb/C material, we cycled the Na–Sb/C half cells with and without the addition of 5% FEC (fluoroethylene carbonate, a surface film forming additive). As shown in Fig. 3, the Sb/C electrode in the FEC-free electrolyte can only be cycled in the first 50 cycles and then failed to give any available capacity after 80 cycles, whereas the Sb/C electrode in the 5% FEC-containing electrolyte can maintain an almost constant capacity of 575 mA h g^{-1} over 100 cycles, exhibiting a superior cycling stability. These very different cycling behaviors can be well accounted for by the effect of FEC electrolyte additive on the structural stability of the solid electrolyte interface (SEI film) on the Sb/C electrode. It is well-recognized that the SEI films formed on the alloy anodes are fragile and easy to damage at repeated cycling, resulting in the continuous creation of fresh surfaces and reconstruction of new SEI films.[15] If these reactions continue to proceed, the SEI films on the anodic alloy particles become thicker and denser, leading to a loss of the electric contact between the electroactive particles and therefore a rapid deterioration of the electrode. Since FEC is an effective electrolyte additive for improving SEI films and cycle life that is frequently used in Li-ion batteries, it may also form a compact SEI film consisting mainly of stable alkali fluoride or fluroalkyl carbonate in the Sb/C anode, which can tolerate the volume changes of the alloy particles at repeated charge and discharge cycles.

To evaluate the effect of FEC additive on the quality of the SEI film, Electrochemical impedance spectroscopic analysis (EIS) of the Sb/C electrode was conducted in the electrolytes with and without the addition of FEC additive and at different cycles of discharge (ESI, Fig. S4 and Table S1†). As shown in Fig. S4a†, the Sb/C electrode in the FEC-free electrolyte displays a continuously enlarged semicircle from the 1st to the 100th cycle, reflecting a gradual increase of the SEI film resistance (R_{SEI}) and the charge transfer resistance (R_{ct}) with increasing cycles. Equivalent circuit simulation of these EIS spectra (Fig. S4c and Table S1) revealed that the R_{SEI} of the Sb/C electrode cycled in the FEC-free electrolyte increased

more than fifty times from 7.7 Ω to 392.8 Ω after 100 cycles, implying a loss of the compactness and a deteriorative change of the SEI film. On the contrary, the R_{SEI} value of the Sb/C electrode in the 5% FEC-containing electrolyte remained almost unchanged at around 25 Ω, suggesting a stable SEI film formed on the Sb/C surfaces. Fig. 3 shows the correlations between the cycling capacity and the SEI resistances of the Sb/C anodes cycled in FEC-free and 5% FEC-containing electrolytes. It is clear from Fig. 3 that the cycling stability of the Sb/C anode depends closely on the structural stability of the SEI film on the Sb/C anode. With improved SEI film, the Sb/C nanocomposite can achieve high capacity and long-term cycling stability as a feasible Na storage alloy anode for Na-ion batteries.

In summary, we prepared a Sb/C nanocomposite simply by mechanical ball-milling commercial Sb powder with conductive carbon. The Sb/C nanocomposite displays a nearly full utilization of its 3 Na-storage capacity, a high initial coulombic efficiency of 85% and a superior rate capability with 50% capacity realized at a very high current of 2000 mA g^{-1}. Particularly, in the optimized electrolyte with a SEI film-forming additive, the Sb/C anode demonstrates a long-term cycling stability with 94% capacity retention over 100 cycles. These excellent electrochemical performances enable the Sb/C nanocomposite to be used as a high capacity and cycling-stable anode for Na-ion batteries.

Notes and references

1 V. Palomares, P. Serras, I. Villaluenga, K. B. Hueso, J. Carretero-Gonzalez and T. Rojo, *Energy Environ. Sci.*, 2012, **5**, 5884–5901.
2 T. R. Jow, L. W. Shacklette, M. Maxfield and D. Vernick, *J. Electrochem. Soc.*, 1987, **134**, 1730–1733.
3 J. Barker, M. Y. Saidi and J. L. Swoyer, *U. S. Pat.*, 2005, 6,872,492.
4 X. Lu, G. Xia, J. P. Lemmon and Z. Yang, *J. Power Sources*, 2010, **195**, 2431–2442.
5 Y. Cao, L. Xiao, W. Wang, D. Choi, Z. Nie, J. Yu, L. V. Saraf, Z. Yang and J. Liu, *Adv. Mater.*, 2011, **23**, 3155–3160.
6 R. Berthelot, D. Carlier and C. Delmas, *Nat. Mater.*, 2011, **10**, 74–80.
7 J. Qian, M. Zhou, Y. Cao, X. Ai and H. Yang, *Adv. Energy Mater.*, 2012, **2**, 410–414.
8 M. Zhou, L. Zhu, Y. Cao, R. Zhao, J. Qian, X. Ai and H. Yang, *RSC Adv.*, 2012, DOI: 10.1039/c2ra20666h.
9 R. Zhao, L. Zhu, Y. Cao, X. Ai and H. X. Yang, *Electrochem. Commun.*, 2012, **21**, 36–38.
10 R. Alcantara, P. Lavela, G. F. Ortiz and J. L. Tirado, *Electrochem. Solid-State Lett.*, 2005, **8**, A222–A225.
11 S. Komaba, W. Murata, T. Ishikawa, N. Yabuuchi, T. Ozeki, T. Nakayama, A. Ogata, K. Gotoh and K. Fujiwara, *Adv. Funct. Mater.*, 2011, **21**, 3859–3867.
12 M. M. Doeff, Y. Ma, S. J. Visco and L. C. D. Jonghe, *J. Electrochem. Soc.*, 1993, **140**, L169–L170.
13 V. L. Chevrier and G. Ceder, *J. Electrochem. Soc.*, 2011, **158**, A1011–A1014.
14 L. Xiao, Y. Cao, J. Xiao, W. Wang, L. Kovarik, Z. Nie and J. Liu, *Chem. Commun.*, 2012, **48**, 3321–3323.
15 S. Komaba, T. Ishikawa, N. Yabuuchi, W. Murata, A. Ito and Y. Ohsawa, *ACS Appl. Mater. Interfaces*, 2011, **3**, 4165–4168.